Reliability of a 13 000-SHS photovoltaic rural electrification programme

Luis Miguel Carrasco , Luis Narvarte, Ana Peral and Manuel Vázquez

ABSTRACT

In this paper, a reliability analysis of a photovoltaic rural electrification (PVRE) programme is proposed considering the failures in the 13 000 installed Solar Home System (SHS) devices occurring over a long operating period of 5 years. A previous arrangement of the database and a brief explanation of the reliability concepts will serve to introduce the failure distribution of every component, from which the SHS lifetime operating features will be described. An application example will show the usefulness of the obtained results in the forecasting of spare parts during the maintenance period. The conclusions of this study may be useful in the scientific design of PVRE programme maintenance structures, with the goal of shedding some light on the technical management mechanisms in decentralised rural electrification.

KEYWORDS

photovoltaic; rural electrification; reliability; failure rates; maintenance

***Correspondence**

Luis Miguel Carrasco, Instituto de Energía Solar, Universidad Politécnica de Madrid, Avenida Complutense s/n, 28040 Madrid, Spain.
E-mail: luismiguel.carrasco@ies-def.upm.es

1. INTRODUCTION

The so-called Solar Home System (SHS) represents a well-proven alternative for decentralised rural electrification, and corresponding programmes have been promoted for many years [1–9] so that there is an estimated number of more than 4 million SHS currently in operation worldwide [10]. Obviously, the reliability of the SHS components is a key factor in the design of sustainable maintenance structures. However, perhaps because of the intrinsic difficulties in gathering data in decentralised frames, the available literature does not offer real data, thus not allowing us to quantify such reliability. This paper attempts to cover this deficiency by presenting the reliability data obtained from 5 years of operation from 13 000-SHS programmes.

This reliability study was carried out with a real and large photovoltaic (PV) electrification programme achieved in Morocco in one of the areas of the Global Rural Electrification Programme (PERG), spread over 136 000 km^2 and affecting about 100 000 people. This programme [11] was promoted by Morocco's Utility ONE (*Office National de l'Electricité*), which entered into a fee-for-service partnership with several private Energy Service Companies (ESCOs) to electrify rural households in several regions of the country. The ESCO is responsible for the marketing, installation and maintenance of solar equipment as well as the collection of user fees during a 10-year period.

The source of data corresponds to Isofoton, one of the PERG ESCOs, which is responsible for the SHS of 12 provinces (see Figure 1); it has more than 80 000 corrective and preventive maintenance data inputs that have been collected between October 2005 and June 2010. The ESCO carries out the maintenance service in its entire area through nine local agencies, which have several teams of technicians who register the data and have a stock of spare parts provided from a central store in Casablanca. The training of technicians was carried out by the ESCO to acquire the basic knowledge on the maintenance failure diagnosis, repairs and concerns of the SHS.

In Figure 1, the geographical distribution of the provinces belonging to the solar PERG programme is shown.

The questions about which of the SHS components break down together with the frequency will be answered by analysing the time distribution of failures of every SHS component throughout 5 years of operation, using concepts of reliability engineering and by determining the reliability function, $R(t)$, the failure rate, $\lambda(t)$, and the mean time to failure (MTTF).

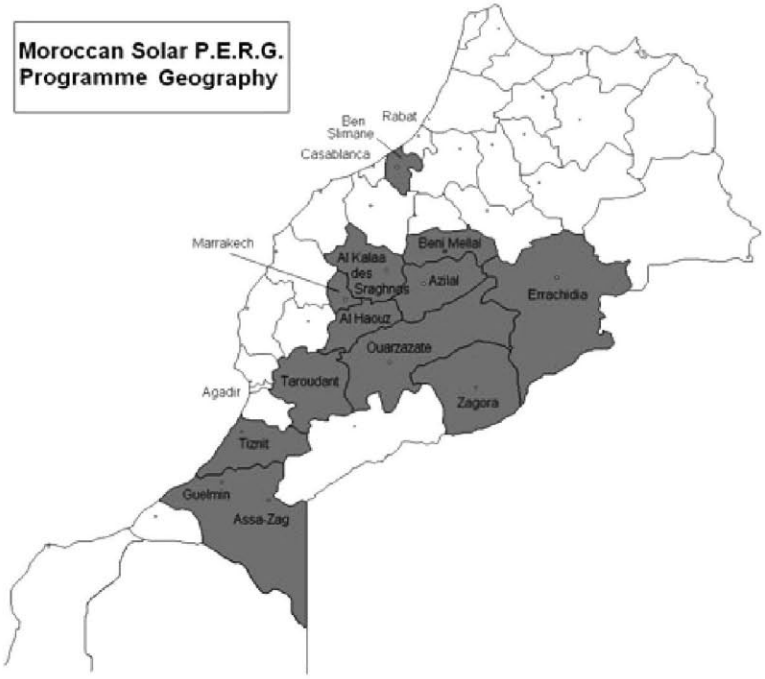

Figure 1. Solar PERG programme geography. Our reliability study was done in the shaded area, which had 13 449 SHS.

2. RELIABILITY ANALYSIS

2.1. SHS components and failure classification

The type of SHS installed in the PERG programme is a standard kit defined by the utility. The programme envisages two different SHS kits to be installed: a 75-W SHS sized to feed four lamps and some small audiovisual devices (TV, DVD, radio, smart-phones chargers, etc.) and a 200-W SHS sized to feed four lamps, some small audiovisual devices and a 160-litre DC refrigerator. However, the 200-W system has not been installed to a large extent (less than 0.14%), and thus it will not be taken into account in the reliability analysis.

The 75-Wp SHS one-line diagram is detailed in Figure 2, and a description of its components is shown in Table I. Note that the PV module power is 80 Wp as a result of its power peak tolerance being $\pm 5\%$. The programme requires a minimum power peak of 75 Wp.

2.1.1. Photovoltaic module

The PV module installed is a 36-series associated monocrystalline cell with a 12-V_{DC} nominal rated voltage. These modules usually have a very high level of reliability, and generally few problems are associated with them. Failures in PV modules can be linked generally to a poorly made electrical contact or a flaw in the bypass diode [12]. It can be noted that module problems are frequently related to a difference between the peak power value shown in the label product and that attained in experimental practice. In any case, this trouble does not involve a failure in the operating system. The expected faults in PV modules are as follows:

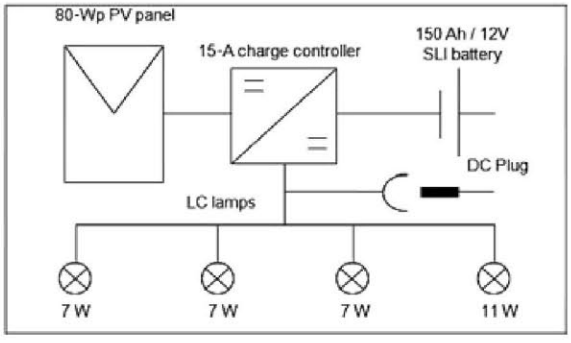

Figure 2. 75-Wp SHS one-line diagram.

- *Diode failures*. This failure can cause a malfunction in the solar module, thus cutting off the operation of some or all PV cells. If a PV module does not work for a few days, the battery will not be charged and the electricity supply will not be available. After some days of an inoperative solar module, the battery self-discharge can give rise to a profound discharge and it will be irreversibly damaged. This battery failure is known in reliability engineering as a secondary failure, as it is caused by the failure of another

Table I. 75-W PERG SHS component description.

Qty	Description	Picture	Qty	Description	Picture
1	80-Wp monocrystalline photovoltaic panel		1	15-A PWM charge controller	
1	150-Ah C_{20} modified SLI battery (12 V)		3 1	7-W_{DC} LC lamp 11-W_{DC} LC lamp	

PWM, pulse width modulation; SLI, starting lighting ignition.

component (main failure). This kind of PV module failure is usually repaired by replacing the damaged diode for a new one; hence, it is a repairable failure.

- *Broken PV module*. Hail, heavy storms, vandalism, etc., can cause PV module breakage, and therefore, it is a catastrophic failure.
- *Thermographic defects*. There are sometimes hotspots in the solar cells, and even in the interconnections between cells (bus), as a result of defects in the manufacturing process, which can be detected by infrared thermographic cameras. The affected cell becomes reverse biassed and dissipates power in the form of heat [13,14], and can destroy the PV module.

2.1.2. Charge controller

The charge controller detailed in Table I uses a pulse width modulation system to charge the battery from the PV module. Its maximum admissible current is 15 A during charge and discharge. This device protects the battery by keeping it working within a prescribed voltage range for an optimal use. It also shows the state of charge (SOC) of the battery by means of some LEDs located at the front of the device, which shows the SOC battery level. The LEDs also warn of system malfunctioning, usually by showing a red LED when deep battery discharge, overload or a short circuit occurs. The charge controller is an electronic device, so its faults occur randomly [12]. This means that the failure rate is constant with time. This behaviour is usually described by exponential distributions of failures, which will be explained later. The failures in this device will be non-repairable (catastrophic failures).

2.1.3. Battery

The accumulator shown in Table I is a 12-V modified starting lighting ignition lead-acid battery. This model is manufactured in Morocco, and its technical report shows a capacity of $C_{20} = 150$ Ah (at 1.8 V minimum discharge voltage per cell and at 20 °C).

The lead-acid battery lifetime is limited by its ageing effects, leading to decreasing capacity and decreasing efficiency, giving rise to higher inner resistance or even to total breakdowns. Sudden failures (catastrophic) can occur in batteries, but they are less significant than failures through continuously ongoing processes. The main causes of ageing are anodic corrosion, sulphatation, degradation of the separator, growth of dendrites and loss of inner surface in the negative electrode [15]. Then, the ageing effect causes degradation failures. According to the standard IEC 60896-11:2002(E) [16], the life cycle of the battery is considered before its residual capacity drops below 80% of its nominal capacity. However, in the real case of field trials, a residual capacity of less than 80% may be a satisfactory battery performance for some users. Some studies indicate that in SHS with 3–4 days of theoretical autonomy, battery degradation will become noticeable (in the sense of less availability of energy) when the useful ampere-hours (Ah) has decreased up to one-third of the nominal battery capacity [17]. The user behaviour with regards to the SHS operation will be closely linked with the battery cycle life.

2.1.4. Low power consumption lamps

The kits include three 7-W_{DC} lamps and one 11-W_{DC} lamp. These devices are made up of a fluorescent tube and electronic ballast. The lifetime for lamps is usually measured as the maximum number of cycles (switch on/off) that lamps can resist. The *Universal Technical Standard for Solar Home Systems* [18] has fixed this resistance to at least 5000 cycles. It may be noted that, unlike the rest of components, lamps have a discrete operation. They do not work continuously, but by cycling. However, we do not consider this difference for the reliability analysis, and we will use the time variable instead of the cycle parameter. The expected failure types in lamps are, on one hand, the random electronic failures in the ballast and, on the other hand, the ageing of the fluorescent tube.

2.1.5. Electrical kit

The SHS electrical installation is made up of wires, light switches, connection box, bulb sockets, a DC plug,

etc., in addition to the devices described above. These components may also be the cause of system failures as a result of manufacturing defects, installation mistakes, etc. However, we do not consider these failures because of a lack of data in the database, but we are aware of the significance of what this SHS failure causes and about the need to study it in more detail.

2.2. The source of data

The database is updated daily from the corrective and preventive maintenance actions carried out by the ESCO technicians. It includes details on the failures of batteries, solar panels, charge controllers and low-power consumption (LC) light lamps for every SHS. These failures are in most cases catastrophic failures, but we must take into account the following considerations:

- The PV module failures resulting from diode breakdowns are considered repaired failures, and not catastrophic failures.
- The batteries replaced by ageing effects are treated as catastrophic failures.

The database also supplies other parameters, such as an identification code for every SHS, the installation date, the dates of preventive and corrective maintenance visits, the location of the system (province, village and geographical coordinates), the broken-down component and its replacement date.

Before the application of the reliability analysis, it was necessary to arrange the database by carrying out a data debugging to remove the invalid inputs, such as mistakes in dates, erroneous PV identification codes or nonrepresentative samples resulting from insufficient data. The database figures, after debugging, are shown in Table II. It is worth noting that the number of SHS considered in the study is still high (7595 after debugging).

We have worked with a very large sample in which there are 44 070 maintenance inputs related to failures, as well as survivors (devices that have not failed during the period considered).

Table II. Recap of the maintenance database after debbugging.

Database	Data inputs after debugging
Number of SHS	7 595
Corrective and preventive maintenance data	44 070
Batteries failed	714
PV panels failed	20
Charge controllers failed	433
7-W lamps failed	2 337
11-W lamps failed	755

2.3. Reliability concepts

The operating life of each component can be determined from the failure database. After 5 years of operation, there are some components that have failed (failure data) and others that have survived (the so-called suspended or right censored data). The failure and suspended data can be used to determine a probability density distribution (pdf) of failures $f(t)$, from which we obtain the cumulative distribution function $F(t)$ [18,19]:

$$F(t) = \int_0^t f(t)dt \tag{1}$$

$F(t)$ is the probability that a component will fail before time $= t$. On the other hand, the reliability function $R(t)$ can be defined as the probability of a component surviving for a time interval. It is given by the complementary expression of the cumulative distribution function $F(f)$:

$$R(t) = 1 - F(t) \tag{2}$$

The failure rate $\lambda(t)$ is the frequency with which a system or component fails. Its function represents the conditional probability of failure in the interval $(t, t + \mathrm{d}t)$ of that component, given that there was no failure before time $\leq t$. It can be expressed as the number of components failing per time unit. Its mathematical expression is as follows:

$$\lambda(t) = \frac{f(t)}{R(t)} \tag{3}$$

Finally, the mean time to failure (MTTF) can be defined as the expected value of time until failure. It measures the average time between failures with the assumption that the failed system is not repaired.

$$\mathrm{MTTF} = \int_0^\infty t \cdot f(t)\mathrm{d}t \tag{4}$$

2.4. Distribution fit

One of the more successful models used in reliability engineering is the Weibull distribution because of its versatility in fitting many different failure models. The Weibull probability density function is shown in Table III.

Depending on the shape parameter β value, the trend of $\lambda(t)$ will be decreasing for $\beta < 1$, constant for $\beta = 1$ and increasing for $\beta > 1$. If $f(t)$ is considered as the pdf of failures, we can obtain the other reliability functions ($\lambda(t)$, $R(t)$ and MTTF) as shown in Table III, where

$\Gamma\left(1 + \frac{1}{\beta}\right)$ is the gamma function $\Gamma(x)$ for $x = \left(1 + \frac{1}{\beta}\right)$

When the β value is close to 1, the reliability distribution approaches an exponential function and the failure rate becomes constant (λ). This distribution is usually a

Table III. Expressions of the probability distribution function [$f(t)$], failure rate [$\lambda(t)$], reliability function [$R(t)$] and mean time to failure [MTTF] for the Weibull, exponential and normal distributions.

Function	Weibull	Exponential	Normal
$f(t)$	$f(t)=\frac{\beta}{\alpha^{\beta}}(t-\gamma)^{\beta-1}e^{-\left(\frac{t-\gamma}{\alpha}\right)^{\beta}}$	$f(t)=\lambda\cdot e^{-\lambda\cdot(t-\gamma)}$	$f(t)=\frac{1}{\sigma\sqrt{2\pi}}e^{-\frac{1}{2}\left(\frac{t-\theta}{\sigma}\right)^2}$
$\lambda(t)$	$\lambda(t)=\frac{\beta}{\alpha^{\beta}}(t-\gamma)^{\beta-1}$	λ	$\lambda(t)=\frac{\frac{1}{\sigma\sqrt{2\pi}}e^{\frac{1}{2}\left(\frac{t-\theta}{\sigma}\right)^2}}{1-\frac{1}{\sigma\sqrt{2\pi}}\int_0^t e^{\frac{1}{2}\left(\frac{t-\theta}{\sigma}\right)^2}\mathrm{d}t}$
$R(t)$	$R(t)=e^{-\left(\frac{t-\gamma}{\alpha}\right)^{\beta}}$	$R(t)=e^{-\lambda\cdot(t-\gamma)}$	$R(t)=1-\frac{1}{\sigma\sqrt{2\pi}}\int_0^t e^{-\frac{1}{2}\left(\frac{t-\theta}{\sigma}\right)^2}\mathrm{d}t$
MTTF	$\mathrm{MTTF}=\gamma+\alpha\cdot\Gamma\left(1+\frac{1}{\beta}\right)$	$\mathrm{MTTF}=\gamma+\frac{1}{\lambda}$	$\mathrm{MTTF}=\int_0^t t\cdot\frac{1}{\sigma\sqrt{2\pi}}e^{-\frac{1}{2}\left(\frac{t-\theta}{\sigma}\right)^2}\mathrm{d}t$

Parameters: α, scale parameter; λ, failure rate; γ, location parameter; θ, mean; γ, location parameter; σ, standard deviation.

good fit for electronic devices, which follow a random model of failures independently of time. The exponential reliability functions are also indicated in Table III, where γ is the location parameter and means that the failure distribution begins at $t=\gamma$. Note that if $\gamma=0$, then MTTF = $1/\lambda$ and $R(t)$ for $t=\mathrm{MTTF}$ is $R(t)=e^{-1}=0.368$. This means that the survival probability for $t=\mathrm{MTTF}$ and $\gamma=0$ is 36.8% [20].

On the other hand, if Weibull's scale parameter $\beta\approx 3.5$, the failure model approaches the normal distribution. It means that there is a dominant failure mechanism, for example ageing, even if other mechanisms intervene in the causes of the failure. The normal functions appear in Table III, where θ represents the mean and σ is the standard deviation. In this case, the survival probability for $t=\mathrm{MTTF}$ is 50%, and the mean θ will have the same value as MTTF [21].

2.5. Failure distribution fit

For obtaining the best fit for a failure distribution, the failure and suspended data need to be put in order and the cumulative probability calculated. The accuracy of this distribution can be improved by calculating the median ranking of cumulative percentages. This approximation can be given by the Bénard estimation [19]:

$$r_i=\frac{i-0.3}{n+0.4} \tag{5}$$

where r_i is the median rank for each failure, i is the ith order failure value and n is the sample size. The median rank is an estimate of the unreliability for each failure.

After the ranking process, the data are ready for plotting to look for the best fit. We will determine how well the data fit an assumed distribution by using some of the many statistical indices that measure the goodness of fit. One of these methods is the least square test. The goodness of fit as derived by this method is the correlation coefficient (ρ). The closer the value ρ is to 1, the better the fit [19].

Once the distribution is defined, the characteristic parameters can be obtained for every distribution and the reliability equations can be solved.

3. ANALYSIS RESULTS

3.1. Fitting distributions

Different fit distributions have been tried for each SHS component, and the following outcomes were obtained:

(i) The charge controller has the best fit with the one parameter ($\gamma=0$) exponential distribution. Figure 3 (a) shows the exponential fit. The two external lines mark the confidence bounds of 95%.

(ii) Low power consumption lamps have the best fit with a two-parameter exponential distribution. Figure 3(b) shows the 7-W_{DC} LC lamp fit, with a confidence level of 95%. Note that the straight line does not start in coordinate (0, 100), but begins at a time before zero ($\gamma=-0.294$ years). This fact is based on the first points appearing at the beginning of the failure distribution on the plot paper following a different distribution, which may be due to an early failure period ($\beta<1$). However, its impact in the fitting result is imperceptible, since the correlation coefficient shows a very high value close to 1. As regards the 11-W_{DC} lamp, it shows the same behaviour as the 7-W_{DC} lamp. It has a location parameter $\gamma=-0.288$ years, and the failure rate figure is 5.97%/year. The two-parameter exponential fit in lamps, in contrast with the one-parameter exponential charge controller fit, can be explained by the fact that the failures in lamps present a residual infant mortality. As shown in the graph, this period is very short, which indicates an acceptable quality control made by the manufacturer.

(iii) The battery has the best fit using the normal distribution. This is coherent with the fact that the main cause of failure is ageing. The correlation coefficient is perceptibly lower than the previous ones, but its figure remains very close to 1. However, there is a range of initial failures that do not fit the normal distribution. In Figure 4(a), we can see that the failures until $t\sim 1.4$ years, out of the normal fit (straight line), have a different tendency. By trying a mixed Weibull distribution, shown in

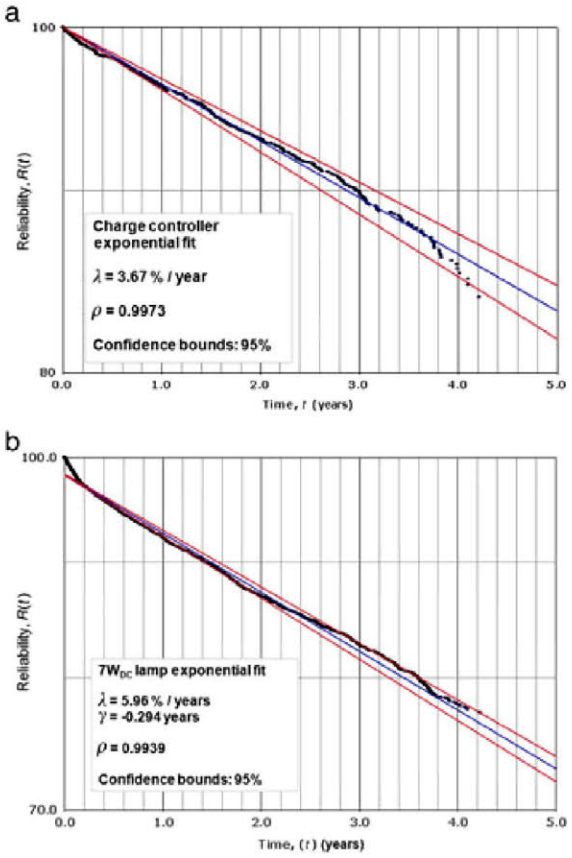

Figure 3. (a) Failure distribution for the charge controller; (b) failure distribution for the 7-W$_{DC}$ LC lamp. Both devices fit for an exponential function (logarithmic scale in the *y*-axis). In the case of the charge controller, the exponential distribution is a one-parameter function. For lamps, the distribution fits a two-parameter exponential model. Both show a very good correlation coefficient (ρ) and a low uncertainty for 95% confidence bounds.

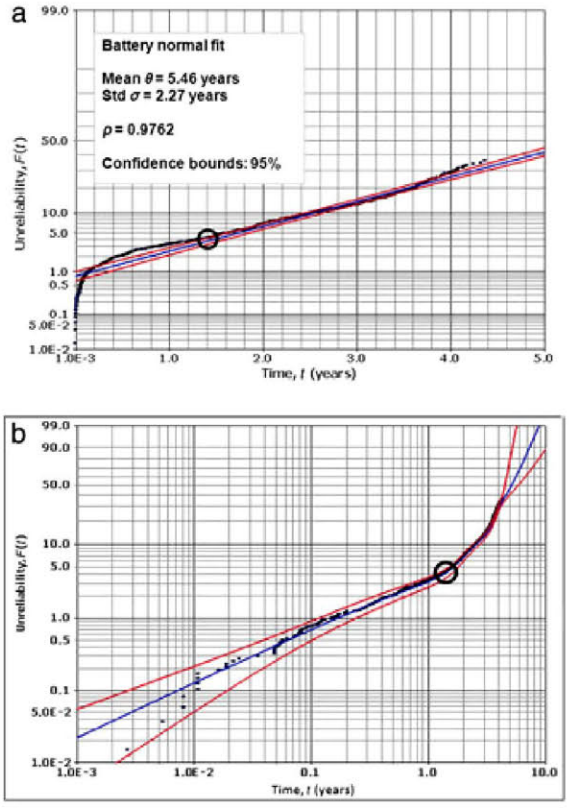

Figure 4. (a) Normal fit of battery failure distribution. The normal probability plot in the *y*-axis represents the cumulative distribution function $F(t)$. (b) Weibull fit. A slope change can be appreciated in the fit distribution line in $t \approx 1.4$ years. The shape parameter β in this stretch line is <1; hence, the failure rate has a decreasing tendency. It is important to note that the failure distribution does not fit exactly the normal function in the first period until 1.4 years. After that, the normal distribution has a high goodness of fit and the correlation coefficient (ρ) presents a figure very close to 1 for the whole fit of failures.

Figure 4(b), we successfully fit the distribution until $t = 1.4$ years with a shape parameter β figure of less than 1. That means that the failure rate during this period decreases over time, that is, the failures are the result of an infant mortality. In what follows, we will maintain the normal distribution as the best fit, although the first-year behaviour has forced us to carry out a more detailed analysis that is currently being done with in-field experiments.

(iv) Finally, the PV panel reliability evaluation was achieved with the data indicated in Table IV.

There have been 20 replacements of PV modules resulting from catastrophic failures. In addition, 20 more failures have been declared although they have not been replaced. After an interview with some of the ESCO maintenance technicians, we found that other different types of PV failures have occurred. The diode failures and hotspots in the cell bus were usually repaired 'informally' by the technicians in the field (they access the cell bus through the tedlar, and then they weld it). The broken PV modules were not replaced because some users did not want to assume the obligation of paying for a new PV module when the breakage was the result of human causes.

After the evaluation of these figures, we concluded that there was not enough information that characterised PV module failures (we only have 40 failure inputs). The evaluation of the failure rate for the PV modules will need more details on the causes of the failure and an in-field analysis of peak power degradation and thermographic analysis. This will be the objective of future work.

3.2. Reliability functions of components and system

The parameters for normal fit (σ, θ) and exponential distribution (γ, λ) were calculated and are shown in Table V. We

Table IV. PV module failure figures: (i) figures from the maintenance database; (ii) some failure information gathered from the maintenance technicians.

PV failures declared in the database	No. of failures	PV failures declared by the maintenance technicians	No. of failures
Replacement but unidentified failures	20	Diode failures	3
Broken PV modules without replacement	5	Breakage of the module through natural causes	9
Unidentified failures; no replacement	15	Breakage of the module through human causes (vandalism)	1
Sum	40	Hot spots at the junctions between cells	6

Table V. Parameters of normal and exponential reliability functions,correlation coefficients and MTTF of the SHS components with 95% confidence bounds.

Parameter			Battery	Charge controller	7-W lamp	11-W lamp
Reliability	Normal	θ (years)	5.46	—	—	—
		σ (years)	2.27	—	—	—
	Exponential	λ (%/year)	—	3.67	5.96	5.97
		γ (years)	—	0	−0.294	−0.288
Goodness of fit		Correlation coefficient (ρ)	0.9762	0.9973	0.9939	0.9954
MTTF (years) ± 95% confidence bound			5.5 ± 3.4%	27.2 ± 9.5%	16.5 ± 4.0%	16.5 ± 7.0%

obtained higher goodness of fit coefficients (ρ) for each one of the fit distributions proposed.

$R(t)$ and $\lambda(t)$ functions were determined from the parameters in Table V and the equations in Table III. We can see in Figure 6 that the reliabilities of 7- and 11-W lamps and charge controller are greater than the battery reliability after the 2nd and 4th operating years. Table V shows that the two lamps have identical failure rates ($\lambda \approx 5.9\%$/year), which are higher than that of the charge controller (3.67%/year). The battery failure rate, however, increases with the time, a typical behaviour when an ageing process is predominant.

The reliability of the system was calculated according to the following series model diagram shown in Figure 5. According to the number of SHS and the failure rate functions shown in Section 3.2, the forecast shown in Table VI was obtained.

It is assumed the SHS is made up of seven independents components. The system fails when one of the components fails. The main goal of an SHS is to provide energy to the loads (lamps and small household appliances). If the PV module or charge controller does not work, the battery will be damaged because of lack of charge or/and deep discharge. If the battery capacity crashes, there will be no energy available to feed the charges; hence, the system fails. As regards the lamps, they are not working in series within the system, but we assumed that when one of the lamps fails because of the lack of service in the room where this lamp worked, then the system fails. Usually, when one lamp fails, a wide area of the dwelling will have an absence of lighting, and we considered this fault as an overall failure of the system. Hence, the proposed SHS model operates according to a series of system lamps.

As regards PV module reliability, it is considered to be close to 1 [22] in order to calculate the SHS reliability function shown in Figure 6 as the product of the individual component probabilities of survival [23]:

$$\begin{aligned} R_{\mathrm{SHS}}(t) &= \Pi R_i(t) \\ &= R_{\mathrm{PV}}(t)\, R_{\mathrm{BAT}}(t)\, R_{\mathrm{CC}}(t)\, R_{7\mathrm{WL}}(t)\, R_{7\mathrm{WL}}(t) \\ &\quad \times R_{7\mathrm{WL}}(t)\, R_{11\mathrm{WL}}(t) \end{aligned} \tag{6}$$

The $R_{\mathrm{SHS}}(t)$ function is plotted in Figure 6. It shows an exponential tendency and a very negative steep slope resulting from the battery function effect. On the other hand, the SHS series failure rate $\lambda_{\mathrm{SHS}}(t)$ function is the sum of the individual component failure rates, as shown in Figure 7:

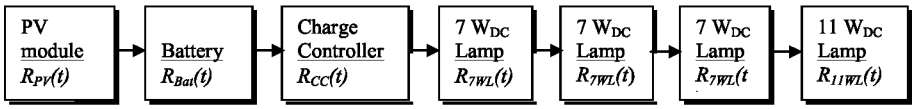

Figure 5. Block diagram representing the SHS series reliability model made up of seven independent components. It is assumed that lamps work in a series model because if one lamp fails, one of the household rooms will not have lighting, and hence the system will have failed.

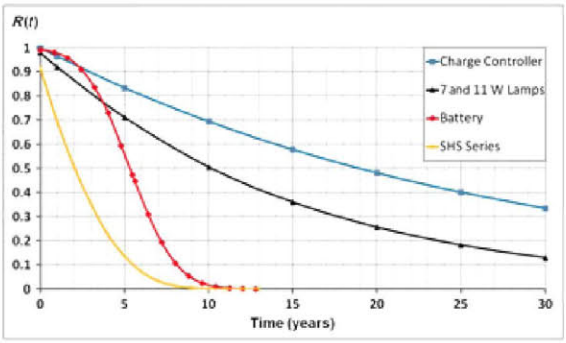

Figure 6. Charge controller, battery, 7- and 11-W lamps and series system (SHS) reliability functions.

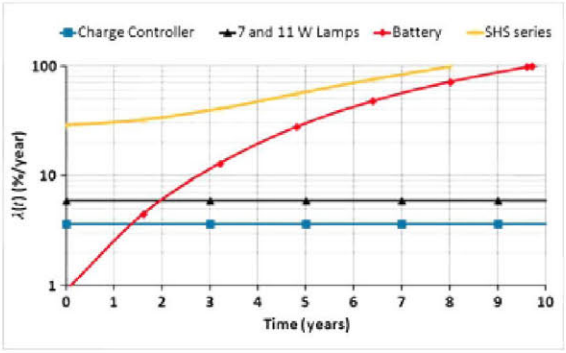

Figure 7. Charge controller, battery, 7- and 11-W lamps and series SHS failure rates.

$$\lambda_{\mathrm{SHS}}(t) = \Sigma R_i(t) = \lambda_{\mathrm{PV}}(t) + \lambda_{\mathrm{BAT}}(t) + \lambda_{\mathrm{CC}}(t) + \lambda_{7\mathrm{WL}}(t) + \lambda_{7\mathrm{WL}}(t) + \lambda_{7\mathrm{WL}}(t) + \lambda_{11\mathrm{WL}}(t) \quad (7)$$

The MTTF for every component is shown in Table V. This parameter was calculated by taking into account a 95% confidence bound [24]. Note that the battery is the component with the lowest MTTF value (5.5 years ± 3.4%), which is in accord with its reliability and failure rate functions. On the other hand, the most reliable component is the charge controller (27.25 years ± 9.5%). The lamps have a very similar MTTF value between them (16.5 years 4% for 7-W lamps and 16.5 years ± 7% for 11-W lamps). It is important to note that the MTTF concept has a different meaning according to the distribution model chosen. In the battery case, whose failure distribution fits a normal model, 5.5 years is the time in which 50% of batteries will have failed. In the case of the charge controller, the MTTF value indicates that 36.8% of devices will have survived after 27.25 years. The case of the lamps, whose distribution model is a two-parameter exponential function, is similar to the charge controller case, except that the location parameter γ intervenes in the MTTF mathematical expression, in accord with the equation in Table III. Therefore, 36.8% of lamps will fail before 16.5 years for both 7- and 11-W_{DC} lamps.

As regards the accuracy of the calculated MTTF, it can be observed that the confidence bounds are very close (less than 10%); therefore, their values have a low uncertainty.

Some authors [25] have studied the mean lifetime of charge controllers and solar batteries based on standard reliability level electronic parts belonging to charge controllers. These studies have concluded with MTTF results of between 30 and 40 years for charge controllers and 6 and 10 years for solar batteries. These theoretical results, based on exponential distributions, are significantly higher than the experimental results shown in this paper, but they may serve as a comparative reference for the MTTF ranges achieved in our study.

4. APPLICATION EXAMPLE

The reliability, and therefore the accumulated cost, of a photovoltaic rural electrification (PVRE) programme is directly linked to the material's repairs and replacements when some of the devices fail. The corrective maintenance in a PVRE programme will need a few technical teams, an optimal stock of spare parts, some vehicles to reach the remote areas where the SHS are located, etc. The ESCO is forced to draw up a forecast for the maintenance period to calculate the optimal stock of spare parts, the number of technical teams and how many vehicles will be necessary, among other things. Then, an application example is proposed using these study results in order to determine the annual stock of spare parts required for a hypothetical 100 000-SHS PVRE programme with a 10-year maintenance period.

According to the number of SHS and the failure rate functions shown in Section 3.2, the following forecast was obtained:

As shown in Table VI, charge controllers and lamps have a constant failure rate, unlike that of the battery's spare parts, which changes every year according to the normal distribution of failures. The annual evolution of the quantities of spare parts is presented in Figure 8.

5. CONCLUSION

This paper details a reliability study that was carried out from a real maintenance database from the 13 000-SHS PERG programme in 12 provinces in Morocco. The failure distribution of every SHS component was evaluated in order to obtain its reliability function $R(t)$, failure rate $\lambda(t)$ and MTTF. The results achieved led to the following conclusions:

- Charge controller and light lamps failure distribution can be established by an exponential function. The two types of lamps (7 and 11 W_{DC}) show an identical

Table VI. Maintenance period forecast for a 100 000-SHS PVRE programme with 10 years of maintenance.

Year	1	2	3	4	5	6	7	8	9	10
Charge controllers	3670 per year									
7-W lamps	17 880 per year									
11-W lamps	5970 per year									
Batteries	2700	5910	10 834	16 704	21 677	23 497	21 801	18582	16 618	16 855

Figures represent the device units required per year.

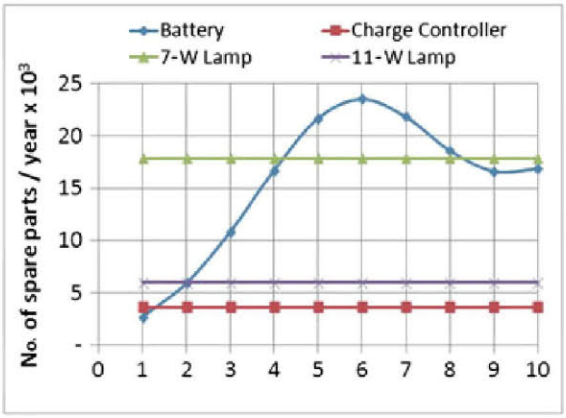

Figure 8. Annual evolution of the spare-part requirements for a 100 000-SHS PVRE programme with 10 years of maintenance.

behaviour as regards their reliability function and failure rate and MTTF parameters.

- Battery failure distribution is better established by a normal function. Although the failures in the first 1.4 years do not fit the normal model exactly, the whole failure distribution has a high goodness of fit, and it presents a correlation coefficient close to 1. In these first 1.4 years, failure distribution fits a Weibull model with a scale parameter β of less than 1; hence, the failure rate in this period has a decreasing tendency. This fact will be analysed for more detailed subsequent studies as regards the batteries installed in the PERG programme.
- As regards the PV modules analysis, the PERG maintenance database does not give enough information about the failure mechanisms of this component. The failures found were 3 damaged diodes, 10 frontal glass breakages and 6 hotpots at the junctions between cells.
- The resulting $R(t)$ and $\lambda(t)$ functions have been shown for each component and for the whole system. It is important to note that battery is the main limiting factor as regards the reliability of the system, since its reliability is much lower than that of the lamps or charge controller.
- The MTTF results show, on the other hand, that the charge controller is the most reliable component (about 27.2 years $\pm$ 9.5%) and the least reliable is the battery (5.5 years $\pm$ 3.4%), while 7- and 11-W LC lamps have a similar MTTF value (16.5 years $\pm$ 4% for 7-W lamps and 16.5 years $\pm$ 7% for 11-W lamps). From these results, we realise again that the battery has a low MTTF value compared with the other components.

These results open the door to characterising the maintenance structure in a PVRE programme. The calculation of the spare-parts stock over a period of 10 years for a 100 000-SHS programme has been shown as an example. It can also be very helpful when a quality improving process needs to be carried out. This study demonstrates that a quality improvement in the battery could raise the system reliability if the battery performance reaches those of lamps or charge regulator.

ACKNOWLEDGEMENTS

We thank Isofoton Maroc s.a.r.l. for its collaboration in this paper by supplying the maintenance database to carry out the present reliability study. This study was partially financed by the Polytechnical University of Madrid.

REFERENCES

1. Rofiqul Islam M, Rabiul Islam M, Rafiqul Alam Beg M. Renewable energy resources and technologies practice in Bangladesh. *Renewable and Sustainable Energy Reviews* 2008; **12**: 299–343.
2. González A, Aritio M, Eyras R, Ngom E. FAD Senegal: program of rural photovoltaic electrification. *Available from* http://www.oecd.org/dataoecd/35/57/ 34966578.pdf, *Internet* 2004.
3. Jacobson AE. Connective power: solar electrification and social change in Kenia. *University of California, available from* http://erg.berkeley.edu/people/AJacobson_PhD_Diss_final04.pdf, *Internet* 2004.
4. Al-Soud MS, Hrayshat ES. Rural photovoltaic electrification program in Jordan. *Renewable and Sustainable Energy Reviews* 2004; **8**: 593–598.
5. Huacuz JM, Flores R, Agredano J, Munguia G. Field performance of lead-acid batteries in photovoltaic rural electrification kits. *Solar Energy* 1995; **55**(4): 287–299.
6. Gunaratne L. Solar photovoltaics in Sri Lanka: a short history. *Progress in Photovoltaics: Research and Applications* 1994; **2**(4): 307–316.
7. Lorenzo E, Aguilera Tejero J. Rural photovoltaic electrification program on the Bolivian high plateau.

Progress in Photovoltaics: Research and Applications 1996; **4**(1): 77–84.

8. Zilles R, Melges de Andrade A, Amaral F. Solar Home System programs in Sao Paulo State, Brasil: utility and user associations experiences. *14th European Photovoltaic Solar Energy Conference, Barcelona* 1997; 931–933.
9. Hansen RD, Martín JG. Photovoltaics for rural electrification in the Dominican Republic. *Natural Resources Forum* 1988; **12**(2): 115 – 128.
10. Camino M. Contribución al aseguramiento de la calidad en la electrificación rural con energías renovables. *Instituto de Energía Solar, Universidad Politécnica de Madrid*, Tesis Doctoral 2011
11. Office National de l'Electricité. Etude des impacts socio-economiques de l'électrification rurale au Maroc. *ONE, available from http://www.one.org.ma, Internet* 2008.
12. Zilles R. A diagnosis on the need to establish a technical requirements protocol for home photovoltaic systems in Latin America. *Energy for Sustainable Development* 1996; **III**(2): 38–43.
13. Muñoz J, Lorenzo E, Martínez-Moreno F, Marroyo L, García M. An investigation into hot-spots in two large grid-connected PV plants. *Progress in Photovoltaics: Research and Applications* 2008; **16**: 693–701.
14. Sánchez-Friera P, Piliougine M, Peláez J, Carretero J, Sidrach de Cardona M. Analysis of degradation mechanisms of crystalline silicon PV modules after 12 years of operation in Southern Europe. *Progress in Photovoltaics: Research and Applications* 2011; **19**(6): 658–666.
15. Bopp G, Gabler H, Preiser K, Sauer DU, Schmidt H. Energy storage in photovoltaic stand-alone energy supply systems. *Progress in Photovoltaics: Research ans Applications* 1998; **6**(4): 271–291.
16. Stationary lead acid batteries - Vented types - General requirements and methods of tests. *International Standard IEC 60896-11*: 2002(E)
17. Díaz P, Egido M, Nieuwenhout F. Dependability analysis of stand-alone photovoltaic systems. *Progress in Photovoltaic: Research and Applications* 2007; **15**: 245 – 264.
18. Universal Technical Standard for Solar Home Systems. Thermie B: *SUP-995-96, EC-DGXVII* 1998.
19. O'Connor PDT. In *Practical Reliability Engineering* (4th edition). Wiley, 2002.
20. Esparza R, Martínez S. Fiabilidad en un sistema de alimentación ininterrumpida. *Mundo Electrónico*, No 48 1976.
21. Warleta J. Fiabilidad. Bases teóricas y prácticas. INTA, 'Esteban Terradas' 1985.
22. Vázquez M, Rey-Stolle I. Photovoltaic module reliability model based on field degradation studies. *Progress in Photovoltaic: Research and Applications* 2008; **16**: 419 – 433.
23. Tobias PA, Trindade DC. In *Applied Reliability* (2nd edn). Chapman & Hall: New York, 1995.
24. Amstadter BL. Reliability Mathematics: Fundamentals, Practices; Procedures. McGraw-Hill: New York, 1971.
25. Mishra PR, Joshi JC. Reliability estimation for components of photovoltaic systems. *Energy Conversion Management* 1996; **37**(9): 1371–1382.